Derivation of the M_n/M_p ratio in exotic nuclei

E. Khan
IJCLab, Université Paris-Saclay, CNRS/IN2P3, 91405 Orsay Cedex, France

(Received 4 October 2021; accepted 20 December 2021; published 5 January 2022)

A generalized formula is provided to calculate the M_n/M_p ratio of the multipole transition matrix elements, in the framework of the so-called phenomenological analysis. It takes into account the possible difference between the neutron and proton radii and diffuseness, which can occur especially in exotic nuclei. The validity domain of the original Bernstein formula is discussed in the case of a proton scattering probe at a few tens of MeV. The largest discrepancies are obtained for very neutron-rich nuclei ($N/Z \gtrsim 1.6$) or when the electromagnetic deformation parameter is larger than the proton scattering one. The reduction of the statistical error bars, and the study of very neutron-rich nuclei at facilities of exotic beams of the new generation, should favor the use of the generalized Bernstein formula.

DOI: 10.1103/PhysRevC.105.014306

I. INTRODUCTION

Information extracted from nuclear excitations can be related to two main quantities: the energy spectrum and the excitation probability. The latter is usually decomposed into a neutron and a proton contribution, leading to the neutron and proton matrix elements, M_n and M_p, respectively [1–3]. The proton one can be directly determined from electromagnetic measurements, such as Coulomb excitation. However, determining the neutron matrix element is more delicate. In practice, another probe is used, such as proton scattering, which involves both protons and neutrons of the nucleus of interest. It is then necessary to combine the electromagnetic and proton scattering data, to extract the M_n and M_p values. With the advent of exotic beam facilities, the M_n/M_p ratio can be now analyzed along several isotopic chains (see, e.g., [4–6]), and provide information about, e.g., modification of the magicity.

In practice, a microscopic analysis is considered the most relevant method to extract the M_n and M_p values. The angular distributions are predicted using optical and transition potentials, involving neutron and proton transition densities. When both the $B(EL)$ and the angular distribution data are well described, the transition densities are validated, providing the M_n and M_p values. Of course, this is an ideal case, since the microscopic transition densities may have to be renormalized in order to describe the data [7,8]. The microscopic approach may also yield some uncertainties, due to the choice of the parameters of both the optical and transition potentials (nucleon-nucleus parametrization, double folding, etc.). The uncertainties on the transition densities should also be considered, such as the validity of assuming them to be spherically symmetric. All in all, it may not be efficient to use a fully detailed microscopic analysis in order to ultimately calculate an integrated quantity, such as M_n or M_p.

Another way to analyze the data is the so-called phenomenological analysis. In this approach, the M_n/M_p ratio is directly determined, assuming a macroscopic behavior for the neutrons and protons of the nucleus of interest. The respective distributions of neutron and proton fluids are deformed due to the excitation [3]. In this method, a phenomenological optical potential is used, such as the Becchetti-Greenlees [9] or Koning-Delaroche [10] parametrization, in the case of proton scattering. The corresponding deformation parameter $\beta_{n,p}$ is determined by normalizing the predicted angular distribution to the data (see, e.g., [7,11–13]). In order to further extract the M_n/M_p ratio, the so-called Bernstein formula [1,2,11] is used, which allows one to relate this ratio to the two deformation lengths, extracted from the electromagnetic probe and a second probe (named hereafter F), such as proton scattering:

$$\frac{M_n}{M_p} = \frac{b_p}{b_n}\left[\frac{\delta^F}{\delta_p}\left(1+\frac{N}{Z}\frac{b_n}{b_p}\right)-1\right] \tag{1}$$

δ is the deformation length corresponding to the electromagnetic (δ_p) or second (δ^F) probe, and relates the transition to the optical potentials, as recalled in the next section. The Bernstein formula also involves $b_{n,p}$, the interaction strength between the external field and a neutron or a proton of the nucleus, respectively.

However, the validity of formula (1) may be limited: it assumes identical neutron and proton radii [1,2], which is not the case in, e.g., exotic nuclei. It has also been known to provide questionable results in several isotopic chains, such as Ar, S, and O isotopes [7,13], although the large statistical error bars, due to the low rate of events with exotic beams, preclude making strong statements.

With the advent of new exotic beams facilities, such error bars are expected to be reduced, and more and more neutron-rich nuclei will be studied. In this framework, and in order to provide a phenomenological extraction of the M_n and M_p values with an extended validity, it could be relevant to generalize the Bernstein formula to the case of exotic nuclei.

 ©2022 American Physical Society

A byproduct is also to provide a derivation of the original Bernstein formula, since I could not find it in the literature. A generalized Bernstein formula could help in providing a quick method to extract the M_n/M_p ratio, including exotic nuclei and isotopic chains.

In Sec. II, the generalized Bernstein formula is derived. Additional hypotheses necessary to reach the original one are discussed, and differences are also analyzed. Section III provides a phenomenological input for the neutron and proton radii and diffuseness, which are necessary to compute, in a convenient way, the generalized Bernstein formula. The comparison of the M_n/M_p ratios, between the original and the generalized Bernstein formulas, is then discussed in the case of 50 MeV/A proton scattering on the S, Ar, and O isotopic chains.

II. THE GENERALIZED BERNSTEIN FORMULA

A. Derivation

In this section, a derivation of the generalized Bernstein formula is provided. The additional hypotheses to reach the original formula are then discussed.

An optical potential U, corresponding to a given probe F interacting with a nucleus, can be decomposed as

$$U = U_n + U_p \tag{2}$$

where $U_{n,p}$ is the contribution to the optical potential from the neutrons (protons) of the nucleus [14].

The transition potential ΔU is generated by the deformation of the nucleus, during the excitation, due to the probe F [14]. The radius R_0 is changed by a quantity, the deformation length $\delta^F \equiv R_0\beta$, where β is the deformation parameter, such that

$$R = R_0 + \delta^F \tag{3}$$

and hence

$$U(R) = U(R_0 + \delta^F) \equiv U(R_0) + \Delta U \tag{4}$$

with

$$\Delta U \simeq \delta^F \left.\frac{dU}{dr}\right|_{r=R_0}. \tag{5}$$

In order to provide a generalization of the Bernstein formula, let us derive the relation between the transition potential and its optical potential, assuming a typical Woods-Saxon shape with potential depth U_0 and diffuseness a, for the latter:

$$U(r) = \frac{U_0}{1 + e^{\frac{r-R_0}{a}}}. \tag{6}$$

This leads to

$$\left.\frac{dU}{dr}\right|_{r=R_0} = -\frac{U_0}{4a} \tag{7}$$

and, therefore, with Eq. (5)

$$\Delta U \simeq -\frac{R_0\beta U_0}{4a}. \tag{8}$$

Equation (2) implies $\Delta U = \Delta U_n + \Delta U_p$, which gives, with Eq. (8),

$$\frac{U_0\delta^F}{a} = \frac{U_p\delta_p}{a_p} + \frac{U_n\delta_n}{a_n}, \tag{9}$$

where $U_{n,p}$ now corresponds to the depth of the neutron and proton contribution to the optical potential, and $\delta_{n,p} \equiv R_{n,p}\beta_{n,p}$. It should be noted that Eq. (9) is a generalization of Eq. (14.124) of [14], taking into account the radius and diffuseness of the potentials.

Equations (2) and (9) allow the calculation of the ratio of the magnitudes of the neutron and proton contributions to the optical potential:

$$\frac{U_n}{U_p} = \frac{\frac{\delta^F}{\delta_p}\frac{a_p}{a} - 1}{\frac{\delta_n}{\delta_p}\frac{a_p}{a_n} - \frac{\delta^F}{\delta_p}\frac{a_p}{a}}. \tag{10}$$

This ratio can also be written using the interaction strength $b_{n,p}$ of a single neutron (proton) of the nucleus with the external probe, as

$$\frac{U_n}{U_p} = \frac{Nb_n}{Zb_p}. \tag{11}$$

Finally, in the framework of the macroscopic model [2,12], the multipole matrix transition elements $M_{n,p}$ are related to the deformation parameters by

$$\frac{M_n}{M_p} = \frac{N}{Z}\frac{\beta_n}{\beta_p}. \tag{12}$$

Equation (12) shows that when M_n/M_p is larger than N/Z, the amplitude of the neutron oscillation, during the excitation, is larger than the proton one, and vice-versa.

Equation (12) allows to write the δ_n/δ_p ratio of Eq. (10) as a function of M_n/M_p, and, together with Eq. (11), provides a generalized expression of the Bernstein formula:

$$\frac{M_n}{M_p} = \frac{b_p}{b_n}\frac{a_n}{a_p}\frac{R_p}{R_n}\left[\frac{\delta^F}{\delta_p}\frac{a_p}{a}\left(1 + \frac{N}{Z}\frac{b_n}{b_p}\right) - 1\right], \tag{13}$$

where $a_{n,p}$ and $R_{n,p}$ are recalled to be the neutron and proton diffuseness and radii, respectively.

B. Reduction to the original Bernstein formula

To recover the original Bernstein formula, it is necessary to assume identical shapes for the total, neutron and proton optical potentials, namely $a = a_n = a_p$ and $R_n = R_p$. In this case, Eq. (13) becomes the usual Bernstein formula (1).

It should be noted that Eq. (13) still assumes identical deformation parameters for the potentials and the densities: β

TABLE I. Parameters (in fm) of the neutron and proton radii phenomenological formulas (14) and (15).

	$A < 40$				$A \geqslant 40$		
	r_0	r_1	r_2	r_3	r_4	r_5	r_6
R_n	1.02	0.75	0.46	1.08	1.18	3.30	0.29
R_p	1.03	0.79	−1.07	0.82	1.24	−0.80	−0.19

TABLE II. Parameters (in MeV for s_1 to s_6) for the phenomenological formula (17) of the neutron and proton separation energies. The value of s_4 in $S_{n,p}$ should be changed by a minus sign in the case of an odd value of N or Z, respectively (pairing effect).

	s_1	s_2	s_3	s_4	s_5	s_6	α
S_n	6.29	3.43	5.85	10.59	1.51	0	−1
S_p	13.83	0.64	3.56	12.14	1.32	0.98	1

of Eq. (8) is assumed to be the same as the one of Eq. (12). It also assumes the validity of the macroscopic model [Eq. (12)].

Compared to the original one [Eq. (1)], the generalized Bernstein formula (13) is more relevant to study the $(M_n/M_p)/(N/Z)$ ratio over isotopic chains involving exotic nuclei, which can have qualitatively different neutron and proton densities.

The specific case $\delta^F/\delta_p = 1$ is useful to illustrate the difference between the original and the generalized Bernstein formulas: the former gives $M_n/M_p = N/Z$, i.e., $\beta_n = \beta_p$, from Eq. (12), whereas the latter still allows for a different deformation parameter between neutrons and protons, due to the possible differences in the shape of the neutron and proton densities.

III. RESULTS

A. Phenomenological implementation

The generalized Bernstein formula (13) involves the proton and neutron radii $R_{n,p}$ and diffuseness $a_{n,p}$. A phenomenological parametrization for these quantities is provided in the present section, in order to use Eq. (13) in a convenient way.

In the case of radii, the following parametrization [15,16] is used, based on the comparison with extensive relativistic mean field (RMF) microscopic calculations. It should be noted that this parametrization has been also validated by comparison with the experimental data, and includes the effect of the isospin dependence.

For light nuclei ($A < 40$) [16]

$$R_{n,p} = r_0 A^{1/3} + r_1 + r_2\left(\frac{N-Z}{A}\right) + r_3\left(\frac{N-Z}{A}\right)^2, \quad (14)$$

where the r_i parameters are given in Table I, for both the neutron and the proton cases. I have taken here the parametrization which is valid for most of the nuclei, but not for the halo ones. The binding energy parameter of the formulas (9) and (10) of Ref. [16] is taken to be 8 MeV. I have checked that taking different values of binding energy, such as 6 MeV, changes the final M_n/M_p value by less that 5%. Finally, it should be noted that the values of the r_i parameters of Ref. [16] are mutliplied by a $\sqrt{5/3}$ factor, due to the relation between the radii and the rms radii (see, e.g., Eq. (10) of Ref. [15]).

For heavier ($A \geqslant 40$) nuclei, the parametrization which best corresponds to the RMF results is [15]

$$R_{n,p} = r_4 A^{1/3} + \frac{r_5 + r_6(N-Z)}{A^{2/3}}, \quad (15)$$

where the r_i parameters, for the neutron and proton cases are also given in Table I.

TABLE III. Ratio of the neutron to proton interaction probability, of a probed nucleus, as a function of the probe [1].

Probe	Energy	b_n/b_p
Electromagnetic	All	0
Protons	10–50 MeV	3
Protons	1 GeV	0.95
Neutrons	10–50 MeV	1/3
α	All	1
π^+	160–200 MeV	1/3
π^-	160–200 MeV	3

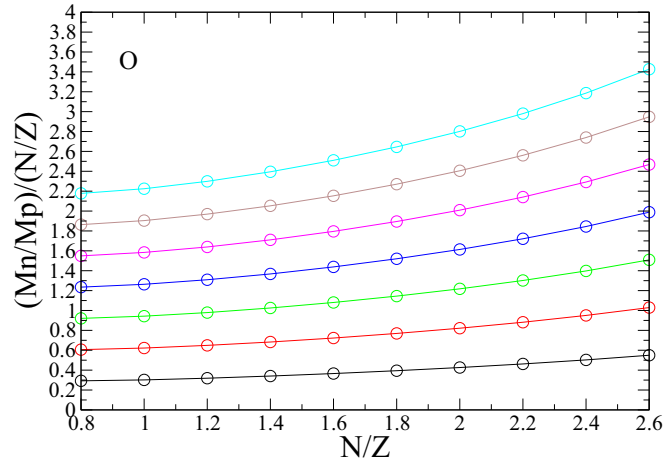

FIG. 1. $(M_n/M_p)/(N/Z)$ ratio calculated with Eq. (13) and the parametrizations of radii and diffuseness from Sec. III A (circles), for δ^F/δ_p ratios ranging from 0.5 to 2 (from bottom to top), with steps of 0.25, in the case of oxygen isotopes.

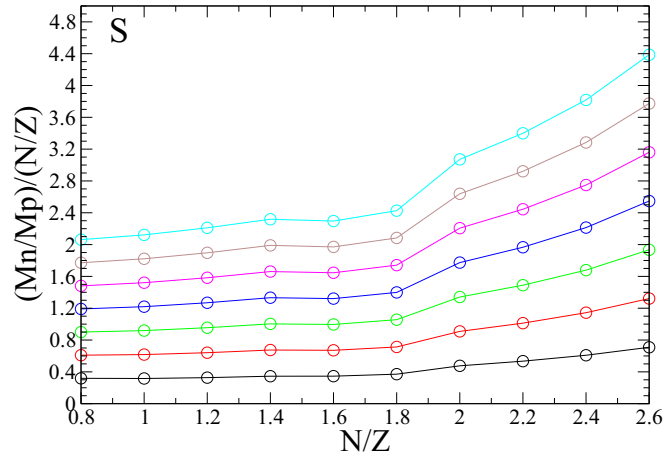

FIG. 2. Same as Fig. 1 but for sulfur isotopes.

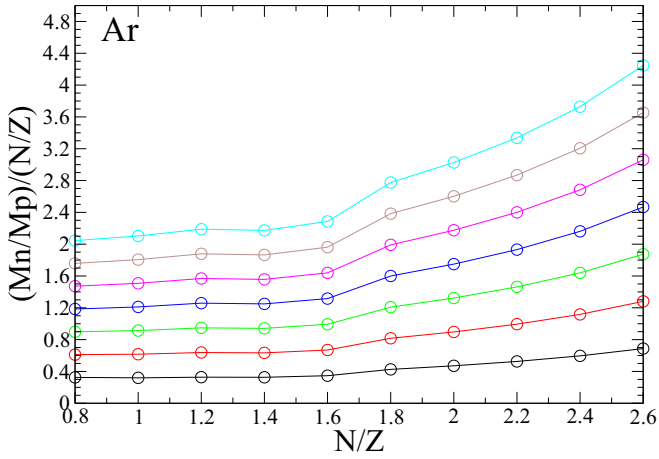

FIG. 3. Same as Fig. 1 but for argon isotopes.

Diffuseness can be related to the separation energy, using [17]

$$a_{n,p} \simeq \frac{\hbar}{2\sqrt{2m_{n,p}S_{n,p}}} \tag{16}$$

It is then relevant to use a parametrization for the separation energy, which has been determined in order to best describe the experimental values [18]:

$$S_{n,p} = (s_1 + s_2 A^{1/3})\left(\frac{N}{Z}\right)^{\alpha} - s_3 + \frac{s_4}{A^{1/2}} - \eta s_5 - s_6 \frac{Z}{A^{1/3}}, \tag{17}$$

where the s_i and α parameters are given in Table II. The η parameter, in Eq. (17), corresponds to the shell correction effect: $\eta = 0$ if the corresponding N or Z value is lower than 28, $\eta = 1$ if this value is between 29 and 50, $\eta = 2$ for a value between 51 and 82, etc.

To summarize, Eqs. (14) and (15) allow the calculation of the R_p/R_n factor of the generalized Bernstein formula (13). Equation (16) provides the values of a_n and a_p, using Eq. (17).

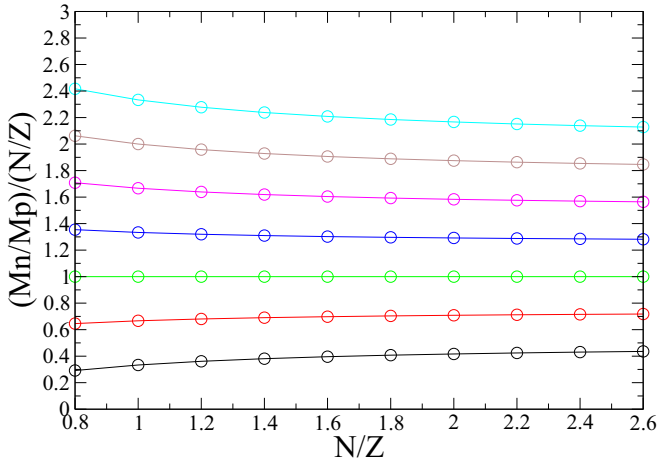

FIG. 4. $(M_n/M_p)/(N/Z)$ ratio calculated with the original Bernstein formula (1) (circles), for δ^F/δ_p ratios ranging from 0.5 to 2 (from bottom to top), with steps of 0.25.

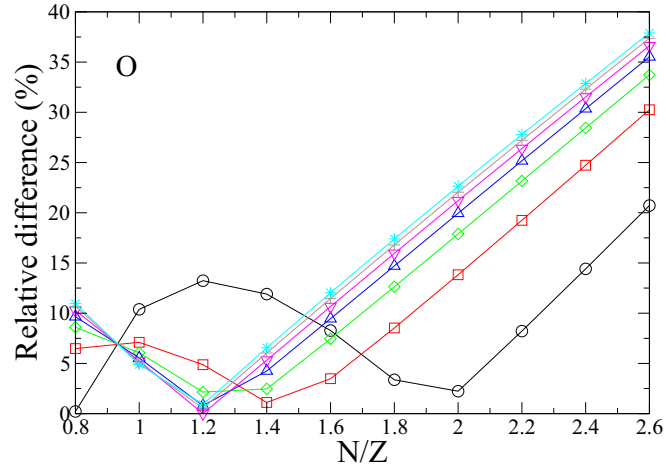

FIG. 5. Relative difference of the M_n/M_p ratios calculated with Eqs. (1) and (13) (symbols), for δ^F/δ_p ratios ranging from 0.5 to 2 (from bottom to top), with steps of 0.25, in the case of oxygen isotopes. See Fig. 1 for the color code.

Finally, the diffuseness a of the optical potential in Eq. (13) is taken to be

$$a = 0.7 \text{ fm}, \tag{18}$$

which is a value close to the one used for the diffuseness of the real part of the phenomenological optical potentials, such as the Becchetti and Greenlees [9] or the Koning and Delaroche [10] ones.

Finally, for a convenient use of Eq. (13), Table III recalls the usual phenomenological values of the b_n/b_p ratio [1,2,11].

B. Results and comparison with the original Bernstein formula

Equation (13) can now be used with the paremeterizations and values provided in Sec. III A for $R_{n,p}$, $a_{n,p}$, $b_{n,p}$, and a. In order to evaluate the impact on the M_n/M_p ratio of the generalization of the Bernstein formula, I consider the case

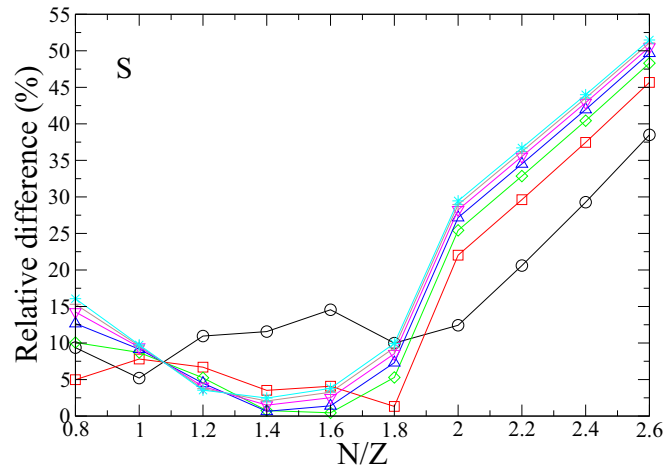

FIG. 6. Same as Fig. 5 but for sulfur isotopes.

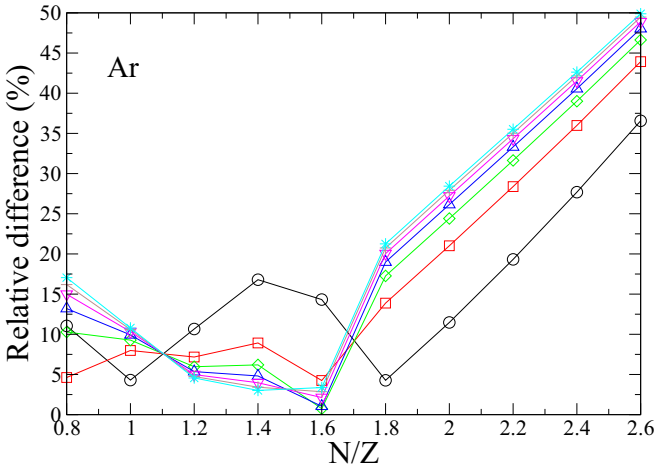

FIG. 7. Same as Fig. 5 but for argon isotopes.

of proton scattering at about 50 MeV/nucleon; the O, S, and Ar isotopic chains have been studied both microscopically and phenomenologicaly [7,13] in this case.

In a first step, the behaviors of the original and the generalized Bernstein formulas are compared, as a function of the $\frac{\delta^F}{\delta_p}$ ratio of the deformations lengths, which are usually determined experimentally. Figures 1–3 display the $(M_n/M_p)/(N/Z)$ ratios, obtained from Eq. (13), for various $\frac{\delta^F}{\delta_p}$ values, in the case of proton scattering at about 50 MeV/nucleon, for the O, S, and Ar isotopic chains, respectively. For comparison, the same ratio using the original Bernstein formula is also plotted in Fig. 4. In this latter case, the calculated M_n/M_p ratio does not depend on the radii and diffuseness of the considered nucleus [see Eq. (1)].

A striking pattern is that the trend of the M_n/M_p ratios, which are rather constant for $N/Z \lesssim 1.6$ and increases for more neutron-rich nuclei with the generalized formula, is not well described by the original Bernstein formula; in this last case, a smooth behavior is obtained, without any strong increase of the M_n/M_p ratio for neutron-rich nuclei. Moreover, Figs. 1–3 exhibit different behaviors among the three isotopic chains. This emphasizes the limitation of the original Bernstein formula, for which an identical behavior is predicted for all nuclei, for given N/Z and $\frac{\delta^F}{\delta_p}$ values.

In order to study more quantitatively the difference between the original and generalized Bernstein formulas, Figs. 5–7 display their relative difference on the three isotopic chains of oxygen, sulfur, and argon, respectively. The largest differences are obtained for very neutron-rich nuclei, with N/Z ratio larger than 1.6 or 1.8, such as ^{48}S and beyond. This result is expected because the original Bernstein formula assumes identical shapes for proton and neutron densities (radius and diffuseness), which is not the case for such neutron-rich nuclei. A more unexpected limitation of the original Bernstein formula impacts nuclei with $N/Z = 0.8$, such as ^{14}O, ^{28}S, or ^{32}Ar. In these slightly proton-rich nuclei, the generalized Bernstein formula leads to variations between 10% and 20% of the M_n/M_p ratio, compared to the original one. Finally, excited states for which δ_p is larger than deformation length δ^F of the probe are also significantly not well described by the original Bernstein formula, namely for $\delta^F/\delta_p = 0.5$ or 0.75.

C. Results from the oxygen, sulfur, and argon data

In a second step, I now compare the M_n/M_p values extracted from the data measured on the first 2^+ states in the oxygen, sulfur, and argon isotopic chains, namely with the electromagnetic probe and the proton scattering one at around 50 MeV per nucleon [7,8,13]. The M_n/M_p ratio is extracted in three different ways: (i) I use the original Bernstein formula (1), from a macroscopic analysis using the Becchetti and Greenlees parametrization of the optical potential [9]. The deformation parameter is obtained by normalizing the theoretical inelastic angular distribution to the data [see, e.g., Eq. (8)]. (ii) The M_n/M_p ratio is also extracted by using the generalized Bernstein formula (13), with the same method. It should be noted that, in these phenomenological approaches, the same radii have been taken for the deformation length of both probes [12] to extract their deformation parameters. (iii) The M_n/M_p values obtained from the microscopic calculation of [7,8,13] are also recalled. In this approach, microscopic transition densities from BCS + QRPA (quasiparticle random-phase approximation) calculations are used with the Jeukenne-Lejeune-Mahaux (JLM) proton-nucleus optical potential [19]. Assuming the shapes of these microscopic densities are relevant, their magnitudes are determined as follows: the proton one, $\delta\rho_p$, from the $B(E2)$ data, and the neutron one, $\delta\rho_n$, using the proton scattering data. The obtained normalization values are then used to microscopically calculate the M_n/M_p ratio, with

$$M_{n,p} = \int \delta\rho_{n,p}(r) r^{L+2} dr, \tag{19}$$

where L is the multipolarity of the excitation (here $L = 2$).

In principle, the better the phenomenological analysis is, the closer the results are to the microscopic values, which are usually considered more sound. However, the microscopic

TABLE IV. $(M_n/M_p)/(N/Z)$ ratios for the sulfur isotopes, calculated with the original Bernstein formula (1), the generalized one (13), and the microscopic analysis of Ref. [7].

$\frac{(M_n/M_p)}{(N/Z)}$	^{30}S	^{32}S	^{34}S	^{36}S	^{38}S	^{40}S
Original	0.93 ± 0.20	0.95 ± 0.11	0.91 ± 0.11	1.13 ± 0.27	1.50 ± 0.30	1.25 ± 0.25
Generalized	0.85 ± 0.18	0.87 ± 0.10	0.88 ± 0.13	1.08 ± 0.34	1.53 ± 0.33	1.26 ± 0.31
Micro	0.88 ± 0.21	0.94 ± 0.16	0.85 ± 0.23	0.65 ± 0.18	1.09 ± 0.29	1.01 ± 0.27

TABLE V. Same as Table IV, but for argon isotopes.

$\frac{(M_n/M_p)}{(N/Z)}$	^{34}Ar	^{36}Ar	^{40}Ar	^{42}Ar	^{44}Ar
Original	1.18 ± 0.25	1.57 ± 0.25	0.75 ± 0.05	1.14 ± 0.17	1.26 ± 0.16
Generalized	1.06 ± 0.21	1.40 ± 0.25	0.68 ± 0.07	1.05 ± 0.23	1.21 ± 0.19
Micro	0.99 ± 0.17	1.41 ± 0.50	0.68 ± 0.21	1.12 ± 0.26	1.13 ± 0.27

analysis also has its own limitations, such as using spherical densities for deformed nuclei, or the limitations of the JLM approach, with a necessary renormalization of the imaginary part of the optical potential [20].

The $(M_n/M_p)/(N/Z)$ values for the sulfur isotopes are displayed in Table IV. The errors bars are determined from the experimental error bars of both the electromagnetic and proton scattering data. The two phenomenological analyses and the microscopic one provide the same trend: an increasing $(M_n/M_p)/(N/Z)$ ratio with increasing neutron number, except in the case of ^{36}S. In this nucleus, the microscopic analysis finds a decrease of the neutron contribution to the excitation, which can be understood from the $N = 20$ shell closure. The generalized Bernstein formula gives a somewhat smaller value than the one from the original formula, but it is not possible to make a strong assessment, because of the error bars. On average, the generalized Bernstein formula gives values closer to the microscopic one than the original formula. In the case of ^{38}S, both macroscopic values are significantly larger than the microscopic one, although compatible within their error bars. It should be recalled that the microscopic analysis is not a straight data value; it also comes with an analysis process and its own limitations.

In the case of the argon isotopes (Table V), the same trend is observed, namely the generalized Bernstein formula gives M_n/M_p values usually closer to the microscopic one than the original Bernstein formula, but the error bars do not allow one to make a strong conclusion. This shows that, in principle, the generalized Bernstein formula is more accurate than the original one, in the sense that the predicted values are closer to the microscopic ones. More accurate measurements, with the upgrade of both detection setups and exotic beam facilities, should provide a reduction of the errors bars, and confirm the usefulness of the generalized Bernstein formulas.

In the case of oxygen isotopes (Table VI), the three analyses are still compatible within the error bars. They all describe a decrease of the neutron contribution, from ^{20}O to ^{22}O, which is interpreted as an $N = 14$ shell closure [8]. The original Bernstein values are at similar level of agreement with the microscopic one, compared to the generalized formula. It could be that, for such light nuclei, the parametrizations described in Sec. II are less accurate. It could also be that the microscopic analysis is not much more accurate than the phenomenological one, in the case of oxygen isotopes. In any case, the difference between the original and the generalized Bernstein formulas is expected to be larger in the case of proton-rich isotopes, such as ^{14}O, as can be seen from Fig. 5, especially if the the electromagnetic deformation parameter is larger than the neutron one.

TABLE VI. $(M_n/M_p)/(N/Z)$ ratios for the oxygen isotopes, calculated with the original Bernstein formula (1), the generalized one (13), and the microscopic analysis of Refs. [8,13].

$\frac{(M_n/M_p)}{(N/Z)}$	^{18}O	^{20}O	^{22}O
Original	1.05 ± 0.13	2.35 ± 0.37	1.28 ± 0.51
Generalized	1.05 ± 0.14	2.60 ± 0.42	1.48 ± 0.63
Micro	0.88 ± 0.19	2.17 ± 0.53	1.4 ± 0.5

More generally, the error bars for all these isotopes are between 10% and 30%; it is difficult to disentangle the results of the generalized Bernstein formula, from the ones of the original formula, as shown on Figs. 5–7. Although the original Bernstein formula does not describe qualitatively the behavior of the M_n/M_p ratio, it describes it quantitatively, because of the still large error bars on this ratio.

IV. CONCLUSION

A generalized formula is provided to derive the M_n/M_p ratio from the deformation parameters obtained from the electromagnetic probe and a second probe, such as proton scattering at a few tens of MeV. It also allows one, in the same way, to rederive the original so-called Bernstein formula: the generalized formula depends on the neutron and proton radii, which were assumed to be identical in the original derivation, as well as on neutron and proton diffuseness.

In order to easily use the generalized formula, phenomenological parametrizations of radii and diffuseness are recalled, which are valid over the nuclear chart. This implementation allows comparison with the original Bernstein formula, in the case of proton scattering at a few tens of MeV per nucleon. The difference is usually less than 10%, except for proton-rich ($N \lesssim 0.8Z$) nuclei, very neutron-rich nuclei ($N \gtrsim 1.5Z$), or for cases where the electromagnetic deformation parameter is larger than the proton scattering one. The original Bernstein formula does not qualitatively describe the behavior of the M_n/M_p ratio of the generalized formula.

The present approach has been discussed using the example of the sulfur, argon, and oxygen data. On average, a better agreement with the microscopic analysis is observed in the case of the generalized Bernstein formula. However, due to current errors bars, and in the case of not too exotic nuclei, the original and Bernstein M_n/M_p ratios are compatible. However, with the increase of the detection capabilities, errors bars are expected to be reduced, and more exotic nuclei should become accessible. This will allow a better assessment of the improvement brought about by the generalized formula.

The validity of the present generalized Bernstein formula has been studied in the case of proton scattering at a few tens

of MeV per nucleon. It would be relevant to also study it for other probes, in a future work, although there is *a priori* no reason that this formula would be less valid in the case of other probes.

ACKNOWLEDGMENT

The author thanks Y. Blumenfeld for fruitful remarks and reading the manuscript, and F. Mercier and O. Sorlin for fruitful discussions.

[1] A. M. Bernstein, V. R. Brown, and V. A. Madsen, Phys. Lett. B **103**, 255 (1981).
[2] A. M. Bernstein, V. R. Brown, and V. A. Madsen, Comments Nucl. Part. Phys. **11**, 203 (1983).
[3] A. Bohr, B. M. Mottelson, *Nuclear Structure* (World Scientific, Singapore, 1998).
[4] S. Calinescu, L. Cáceres, S. Grévy, O. Sorlin, Z. Dombrádi, M. Stanoiu, R. Astabatyan, C. Borcea, R. Borcea, M. Bowry, W. Catford, E. Clément, S. Franchoo, R. Garcia, R. Gillibert, I. H. Guerin, I. Kuti, S. Lukyanov, A. Lepailleur, V. Maslov *et al.* Phys. Rev. C **93**, 044333 (2016).
[5] A. Kundu, S. Santra, A. Pal, D. Chattopadhyay, R. Tripathi, B. J. Roy, T. N. Nag, B. K. Nayak, A. Saxena, and S. Kailas, Phys. Rev. C **99**, 034609 (2019).
[6] M. L. Cortès, P. Doornenbal, M. Dupuis, S. M. Lenzi, F. Nowacki, A. Obertelli, S. Péru, N. Pietralla, V. Werner, K. Wimmer, G. Authelet, H. Baba, D. Calvet, F. Château, A. Corsi, A. Delbart, J.-M. Gheller, A. Gillibert, T. Isobe, V. Lapoux *et al.*, Phys. Rev. C **97**, 044315 (2018).
[7] E. Khan, T. Suomijärvi, Y. Blumenfeld, Nguyen Van Giai, N. Alamanos, F. Auger, E. Bauge, D. Beaumel, J. P. Delaroche, P. Delbourgo-Salvador, A. Drouart, S. Fortier, N. Frascaria, A. Gillibert, M. Girod, C. Jouanne, K. W. Kemper, A. Lagoyannis, V. Lapoux, A. Lépine-Szily *et al.* Nucl. Phys. A **694**, 103 (2001).
[8] E. Becheva, Y. Blumenfeld, E. Khan, D. Beaumel, J. M. Daugas, F. Delaunay, Ch.-E. Demonchy, A. Drouart, M. Fallot, A. Gillibert, L. Giot, M. Grasso, N. Keeley, K. W. Kemper, D. T. Khoa, V. Lapoux, V. Lima, A. Musumarra, L. Nalpas, E. C. Pollacco *et al.* Phys. Rev. Lett. **96**, 012501 (2006).
[9] F. D. Becchetti and G. W. Greenlees, Phys. Rev. **182**, 1190 (1969).
[10] A. J. Koning and J. P. Delaroche, Nucl. Phys. A **713**, 231 (2003).
[11] P. D. Cottle, Nucl. Phys. A **682**, 124c (2001).
[12] M. A. Kennedy, P. D. Cottle, and K. W. Kemper, Phys. Rev. C **46**, 1811 (1992).
[13] E. Khan, Y. Blumenfeld, Nguyen Van Giai, T. Suomijärvi, N. Alamanos, F. Auger, G. Colò, N. Frascaria, A. Gillibert, T. Glasmacher, M. Godwin, K. W. Kemper, V. Lapoux, I. Lhenry, F. Maréchal, D. J. Morrissey, A. Musumarra, N. A. Orr, S. Ottini-Hustache, P. Piattelli *et al.* Phys. Lett. B **490**, 45 (2000).
[14] G. R. Satchler, *Direct Nuclear Reactions* (Clarendon, Oxford, 1983).
[15] M. Warda, B. Nerlo-Pomorska, and K. Pomorski, Nucl. Phys. A **635**, 484 (1998).
[16] J. S. Wang, W. Q. Shen, Z. Y. Zhua, J. Feng, Z. Y. Guo, W. L. Zhan, G. Q. Xiao, X. Z. Cai, D. Q. Fang, H. Y. Zhang, and Y. G. Ma, Nucl. Phys. A **691**, 618 (2001).
[17] Y. K. Gambhir and S. H. Patil, Z. Phys. A **321**, 161 (1985).
[18] K. Vogt, T. Hartmann, and A. Zilges, Phys. Lett. B **517**, 255 (2001).
[19] J. P. Jeukenne, A. Lejeune, and C. Mahaux, Phys. Rev. C **16**, 80 (1977).
[20] F. Petrovich, S. K. Yoon, M. J. Threapleton, R. J. Philpott, J. A. Carr, F. S. Dietrich, and L. F. Hansen, Nucl. Phys. A **563**, 387 (1993).